APL-UW Field-Scale Axial Flow Turbine: Design and Specifications

Christopher Bassett, Justin Burnett, Katherine Van Ness, Harlin Wood, Jesse Dosher, Ben Cunningham, Jessica Noe, and Tracy Tran

Technical Report

APL-UW TR 2402

Septemember 2024

Applied Physics Laboratory
1013 NE 40th Street

University of Washington
Seattle, Washington 98105-6698

ACKNOWLEDGMENTS

This work was supported by U.S. Naval Sea Systems Command (NAVSEA) under contracts N00024-18-F-8702 and N00024-21-D-6400. We acknowledge the contributions of Brian Polagye and Andy Stewart, who both had a role in project administration during the design and fabrication stages.

ABSTRACT

Axial flow turbines designed to generate power from underwater currents (tidal and riverine) are similar to the commonly observed wind turbines. With support from U.S. Naval Sea Systems Command, engineers at the Applied Physical Laboratory of the University of Washington (APL-UW) have designed and fabricated a one-meter diameter axial flow turbine for use in APL-UW's marine energy research program. The system, referred to as the AFT (axial flow turbine), is designed for deployment from R/V *Russell Davis Light*, where the vessel, under propulsion, is used to simulate naturally occurring currents for power generation. This report summarizes the AFT's mechanical and electrical design and is intended as a reference to support research efforts performed using the system. Encoders and six-axis load cells installed on the driveshaft and at the root of one of the rotor's three blades, allow for characterization of the forces and torques generated during operation. The system was designed for reliability and to acquire scientific-quality data to advance studies of axial flow turbines. Thus, system components selected in the design process are not intended to maximize system efficiency and power extraction.

CONTENTS

LIST OF TABLES

LIST OF FIGURES

1 MOTIVATION

The University of Washington (UW) has a robust research and development program focused on horizontal and vertical axis current energy turbines. This research is performed at the laboratory scale using the Alice C. Tyler Flume installed in the Harris Hydraulics Laboratory, while field-scale research is performed using the Applied Physics Laboratory's R/V *Russell Davis Light* (RDL). Research and development of projects performed at UW represent collaborations between the Mechanical Engineering, Civil and Environmental Engineering, and Aeronautics and Astronautics departments while APL-UW's primary role has been focused on design and fabrication of systems to support this work.

As part of UW's current turbine research and development program, a laboratory-scale axial flow turbine (AFT) was developed for flume studies, which has been used to investigate active and passive adaptive blade pitch control strategies.[1–3] While a research tool, a fundamental limitation of systems designed for experiments in the tank is the size restriction. Tank size limits the size of blades that can be tested. Driven by some of the practical limitations imposed by this testing, APL-UW developed an axial flow turbine system that allows for larger geometries (less than 1.5 m diameter rotors) to be tested. While small compared to grid-scale applications, rotors on the order of a meter in diameter have the potential to provide power to smaller loads in remote areas lacking permanent infrastructure, thereby catalyzing new developments in industry, sensing capabilities, and power generation for autonomous vehicles.

Testing of AFT, and other small-scale current turbines, is performed under propulsion in Lake Washington using RDL's unique characteristics. Specifically, the research vessel is equipped with a gantry permanently installed near the bow of the vessel (Fig. 1). Turbines can be mounted on custom frames, which are lowered into the water column, well clear of any obstructions associated with the vessel. By maneuvering the vessel under propulsion it is then possible to operate field-scale systems, including AFT, at currents up to 2.5 m/s without the size and confinement restrictions of the tank. Lake Washington, located just east of the University of Washington campus, is approximately 20 miles long, so tests under propulsion can be carried out for long periods while the vessel maintains constant speed and heading. This approach minimizes the variability in inflow conditions that would be associated with regular modifications to operational conditions during testing.

This report provides a high-level summary of the system's design and specifications, and presents

preliminary AFT test results from experiments on Lake Washington. Note that the system was designed as a research and development tool, and not to maximize power generation. Thus, numerous aspects of the system's design were therefore selected not to maximize efficiency but to reduce component costs or minimize the probability of failure during testing. Some of these design trade-offs could have notable negative consequences were the primary research objective performance with respect to power generation (e.g., numerous redundant seals increase losses in the system but decrease the probability of water intrusion between maintenance). To close the gaps between mechanical power associated with the lift and allow this to be effectively translated into power production potential, the system is equipped with multiple load cells and encoders so that relevant dynamics variables can be measured.

Figure 1: R/V *Russell Davis Light* with the AFT installed (without blades). The plume frame on which the AFT is mounted is lowered into the water during testing.

2 SYSTEM DESCRIPTION

The field-scale AFT has a three-blade design with a rotor diameter of 1 m. Overall length is 2.05 m and outer diameter of the system aft the rotor is 0.24 m. The system is designed to accommodate inflow speeds up to 2.5 m/s with maximum rotor torques of 120 N m, maximum thrust loads of approximate 6800 N (with the load cell, not the bearings, being the limiting factor), and rotor rotation rates up to 260 revolutions per minute (RPM).[a] The following sections summarize the design and specifications of AFT subsystems with the exception of the blades. A description of the system's blades is omitted because the system is designed specifically to accommodate different blades for research and development purposes. Thus, blades and their impacts on system performance are the focus of work using this system.

As designed, the turbine is deployed underwater while critical components for operations and controls are contained in an air-side enclosure (Fig. 2). Custom software installed on a desktop computer is used for system control and data acquisition. The electronics enclosure (Sec. 2.1), which receives 120 Vac plus 240 Vac power from RDL and communicates with the desktop computer Ethernet, is installed in the laboratory space on the research vessel. While drawn as a single unit (Fig. 2), the AFT is broken into multiple parts: the hub, the nacelle, and the motor housing. This modular design facilitates fabrication, assembly, and bench-top testing. With the exception of the shroud for the flooded section, the body of the unit is assembled from hard anodized 6061 aluminum components. The system is designed for use in fresh water so it is equipped with magnesium anodes.

Multiple underwater cables equipped with wet-mate SubConn connectors support power and communications from the air-side components to the turbine. All connection points are located at the downstream end of the nacelle where they are shielded from the external flow and protected by the frame of the Nacelle. From the connectors communications and power are distributed throughout the underwater subsystems as described in Sections 2.2 and 2.3.

2.1 Air-Side Electronics

The air-side electronics enclosure (Figs. 3 and 4) contains all of the equipment necessary to communicate with and operate the AFT with the exception of a desktop computer, network switch,

[a] Higher rotation rates, potentially up to 340 RPM, will be achievable with a new fixed pitch rotor design now in development.

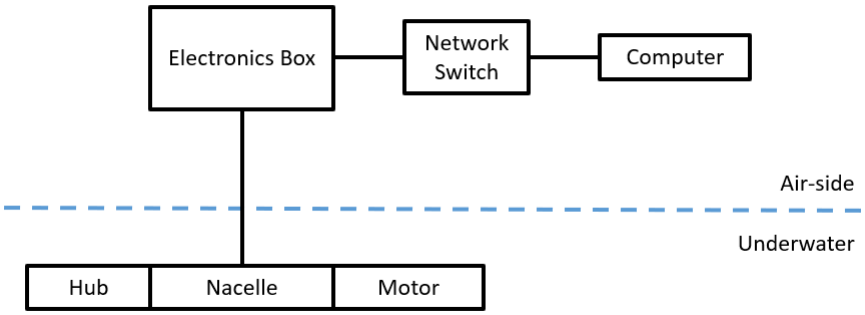

Figure 2: Simple block representation of the field-scale axial flow turbine subsystems.

and load dump resistors installed in a separate frame. The enclosure receives both 240 Vac, three-phase and 120 Vac, single-phase power. Following a circuit breaker, the 240 Vac is supplied directly to a variable frequency drive (VFD; TECO Westinghouse E510) used to operate and control the AFT well pump motor (generator) during testing. Power generated by the system during operation is dissipated by the load dump resistors connected to the VFD. A parallel circuit includes a 48 Vdc power supply used to drive the blade pitch motor controllers (Maxon EPOS4 Compact 50/15 smart positioning control units) installed in the hub of the AFT.

All components of the system are controlled by a Versalogic BayCat PC/104-*Plus* computer and associated power supply board and ancillary controller area network (CAN) Bus board. An external RLS E201-9Q quadrature encoder interface interprets RS-422 level-signals and passes a count to the computer to enable tracking of the angular position of the shaft. Rotor rotation rate is driven by the VFD, which can be driven either directly by commands from the PC/104 stack or by manually manipulating the controls on the drive. System controls from the PC/104 are provided by remotely connecting to the computer from an external desktop personal computer using secure shell protocol (SSH) and a custom user interface. An analog to digital/digital to analog converter (ADC-DAC) board is also installed in the air enclosure and interfaces with a temperature sensor installed in the AFT.

The 120 Vac line drives 12 Vdc and 24 Vdc power supplies. Intake and exhaust fans for temperature control of the enclosure are driven by the 12 Vdc power supply while the 24 Vdc power supply drives a Versalogic PC/104-*Plus* computer, its power supply, an ADC-DAC interface, and CAN bus. The ATI load cell interface boards (ATI F/T CAN Bus Network Interface) are also powered by the 24 Vdc bus. Collectively, these control and acquire data from the pitch motor encoders,

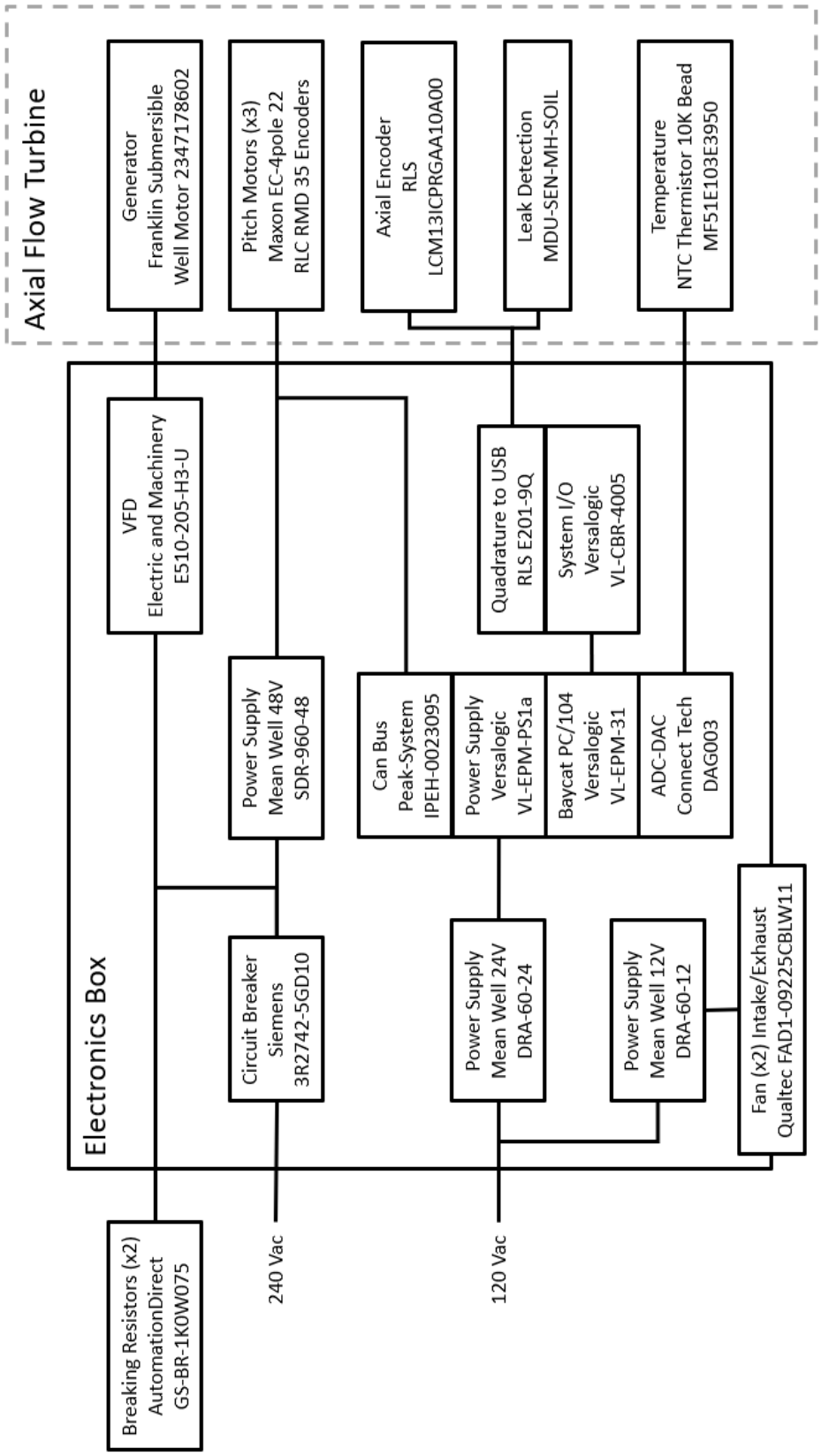

Figure 3: Block diagram summarizing the components and electronic configuration of the AFT system.

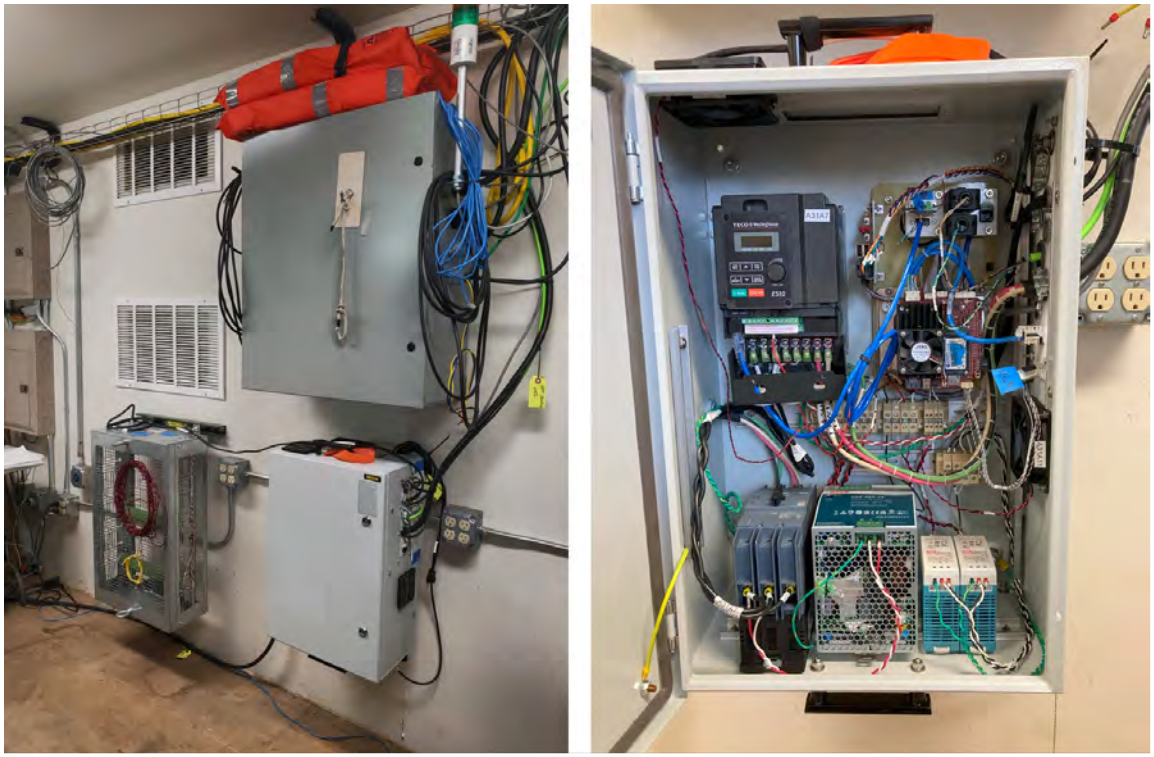

Figure 4: (left) The electronics enclosure and load dump installed in the lab on R/V *Russell Davis Light.* The AFT enclosure is the unit located lower on the wall. Cables exiting the electronics box are routed through the container walls to the gantry/frame where they are secured to AFT's support structures.

primary shaft encoder, leak detection sensor, and a temperature sensor.

Under many test conditions the AFT generates power that is not conditioned or passed back to any local grid or storage system. Instead, the unit is designed to dissipate any power generated by the system with a resistor bank. Up to nine resistors can be installed, in series or parallel, with the AFT configuration including two 75 Ω, 1000 W resistors in parallel. This is more than adequate to dissipate the power generated by the AFT. The breaking resistors are installed adjacent to the electronics enclosure (Fig. 4) in the lab.

2.2 AFT: Nacelle

The nacelle, which we define as the full length of the system aft of the hub, is composed of three sections (Figs. 6 and 7). The forward section provides a connection point between the hub and nacelle, which is composed of a tapered shaft with a hollow interior. This hollow section provides a

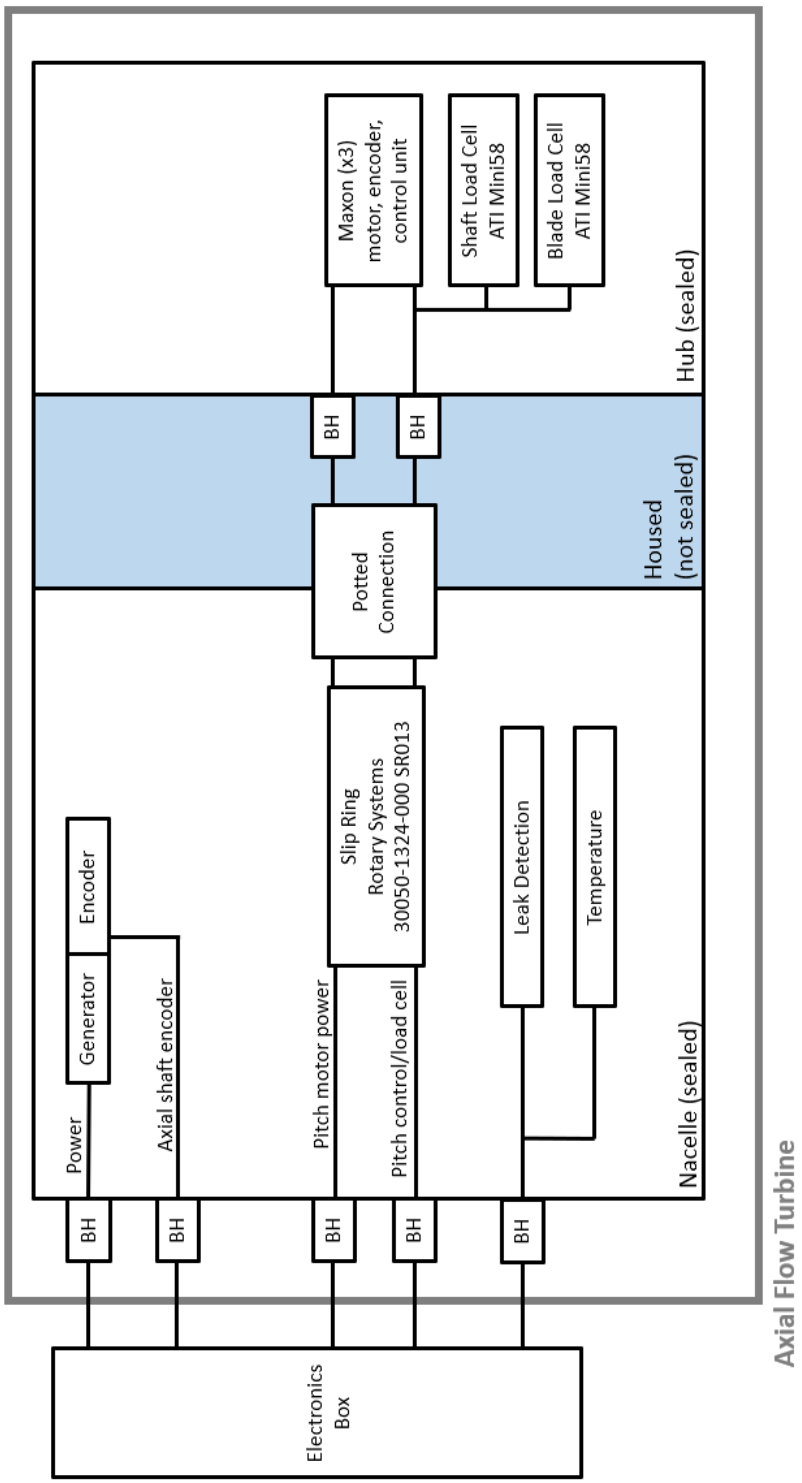

Figure 5: Block diagram of the AFT electrical components. The abbreviation BH denotes bulkhead connectors installed on the AFT.

cable pass (Fig. 6) between the flooded section immediately aft of the hub and the critical electrical components housed in the nacelle aft of the bearing pack. After installation of the cables, the shaft is potted to prevent water intrusion into the nacelle through the shaft because the forward section is flooded during operations. This forward portion of the nacelle is enclosed by a two-part cylindrical polymer (Delrin) housing.

The second portion of the nacelle is housed within the cylindrical anodized aluminum section equipped with redundant o-rings. This section is the area between the bearing housing and shaft coupling (Fig. 6) and this section of the housing, prior to assembly, is shown in the upper left-hand side of Fig. 7. The bearing pack at the forward end of this section has an external mechanical seal (Fig. 8). The shaft is secured by two tapered roller bearings, each adjacent to a lip seal, and a retaining nut. The nacelle carries out two primary functions for the system: management of electrical signals and the transfer of mechanical power from the rotor/hub to the generator. Communications signals and data entering the nacelle connect to a 24-channel slip ring. In Fig. 6 the cables from the nacelle can be seen exiting the shaft and connecting to the forward side of the slip ring. Aft of the slip ring at the end of this section of the hub connects to various SubConn underwater bulkhead connectors. Mechanical power transfer occurs just aft of the slip ring where a shaft (Lovejoy) coupling connects to a 10:1 planetary gearbox mounted just forward of the section's endcap. Forward of the gearbox the shaft rotation rate is measurement by an RLS LM13 contactless high-speed incremental quadrature encoder.

The final section of the nacelle houses the generator while the remaining open portions of the section provide space for the bulkhead connectors and cables running to the air-side electronics enclosure. The generator is a 5 HP, 240 Vac three-phase Franklin submersible well pump. While the system was designed around this well pump motor, which does not require a submersible housing, the generator has been enclosed in a static housing. This choice reflects the potential for water intrusion around the high-speed shaft (up to 2600 RPM) seals between the generator and the main nacelle housing. As with the other components, this entire section is machined from anodized aluminum. The outer dimension matches those of the other AFT sections while the motor housing has a smaller diameter that accommodates both the motor and the o-rings to seal its enclosure. Large holes have been machined in the sides of the outer portion of the unit to facilitate assembly and cable runs.

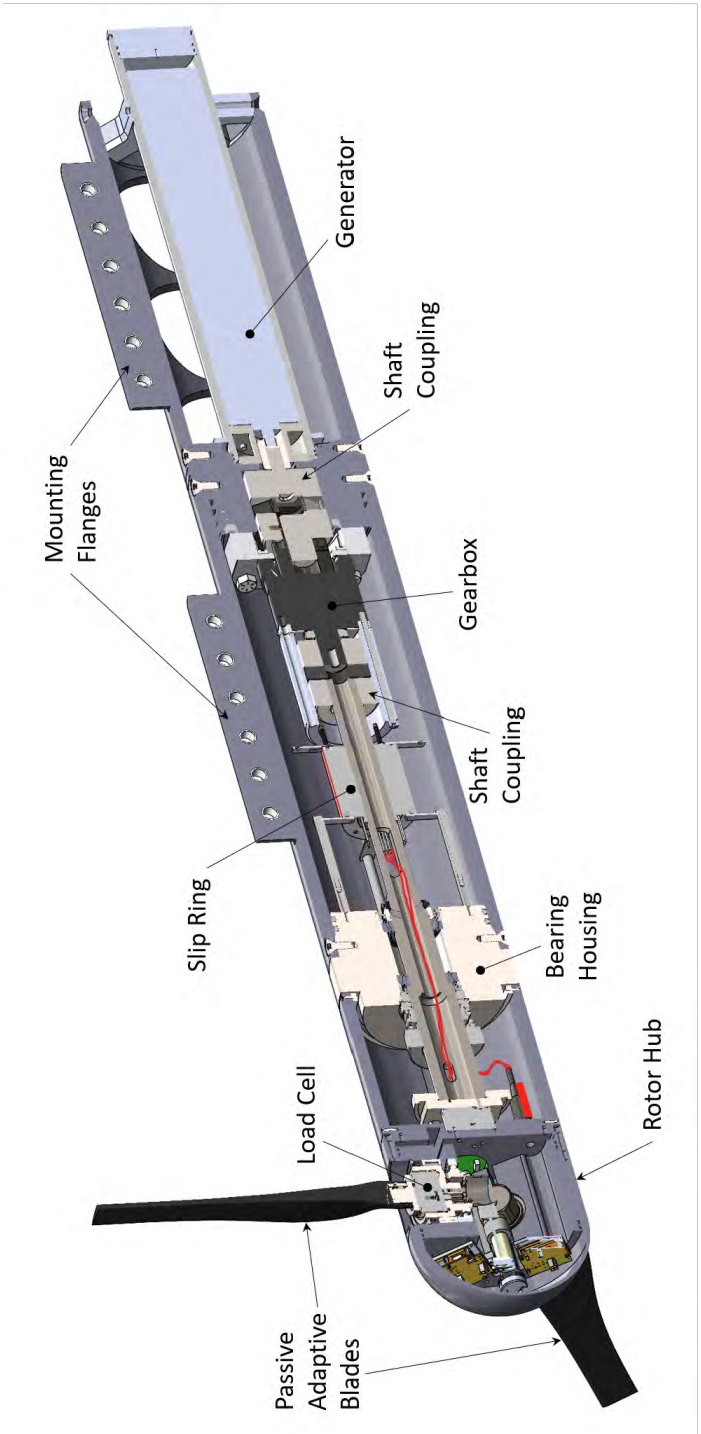

Figure 6: A labeled cross-section of the AFT showing the full assembly and its components. Images of these components prior to assembly are shown in Fig. 7. The red line leading from hub and into the housing with the slip ring, shaft coupling, and gearbox represents the cables transmitting power and data to/from the hub.

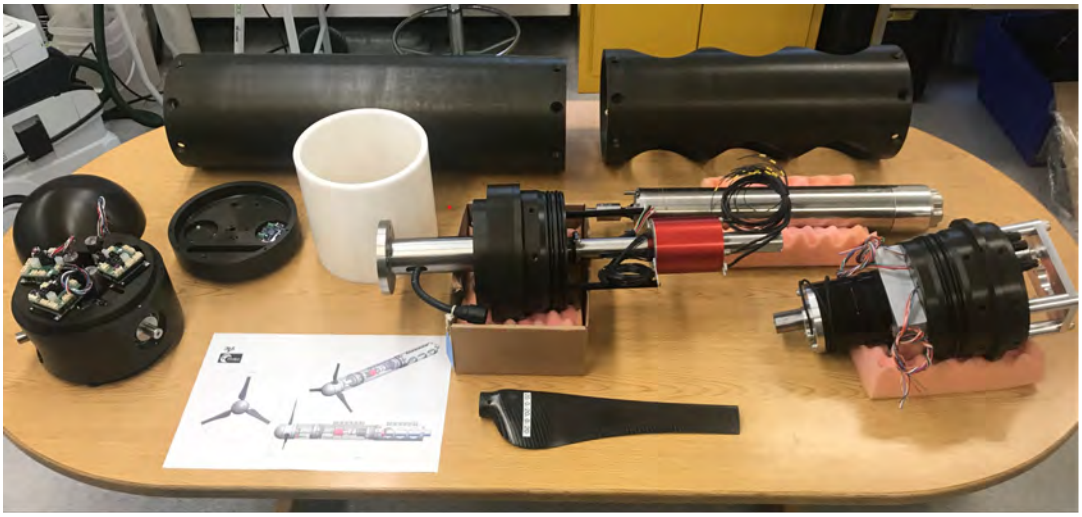

Figure 7: An image of the AFT components prior to assembly. The components are laid out with those located forward on the system being on the left side of the image. The housings are located near the top of the images.

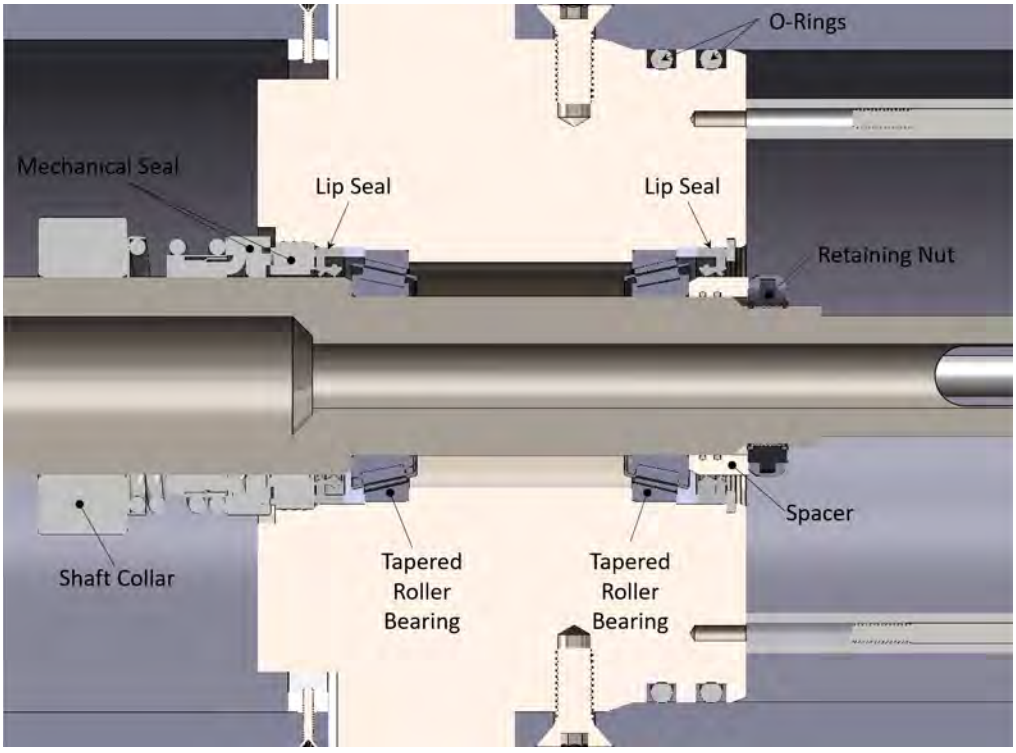

Figure 8: A cross section of the AFT shaft/bearing pack at the forward end of the nacelle.

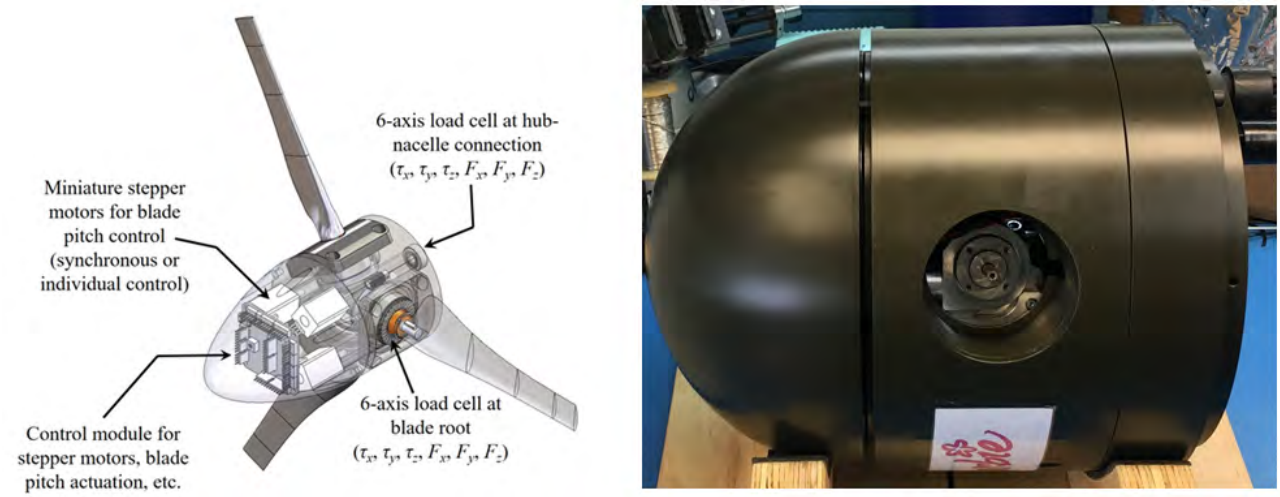

Figure 9: Note the image on the left is not consistent with the final component selection and design, but its annotations are consistent with the capabilities of the unit.

2.3 AFT: Hub

The hub of the AFT is the most compact and complicated subsystem. Contained in the small package are three motors, gearboxes, and control modules that are collectively used to independently control the pitch of each of the AFT's rotor blades (Fig. 9). As implemented, the pitch motors can be controlled with a resolution of 0.1°. At the base of one of the three blades, there is a six-axis load cell for measuring loads on the blade. The exterior of the forward end of the hub is a machined aluminum hemisphere with diameter 0.16 m (6.3 in). Housed in the hub are three Maxon brushless DC motors and associated motor controllers used to control blade pitch. These components are mounted to an aluminum end plate where it sits within the hemisphere. Where the hemisphere meets with the back section of the nacelle, the inner surface is machined to allow for two o-rings to seal this surface.

The back portion of the hub consists of two components. The first is a 0.16 m (OD) aluminum cylinder that has been machined to support the complex installation of a set of shafts, seals, and 90-degree 31:1 spiroid gearboxes and encoders between the Maxon pitch control motors and the blade shafts. The spiroid gearboxes cannot be back-driven, thereby limiting the potential for the blade pitch to slip under load. The three stainless steel shafts, which protrude from the nacelle, have a 1/4-inch wide key way. The blades designed to mount to these shafts have machined collars installed in the roots that slide over the shafts and installed keys requiring only a single 3/16-inch

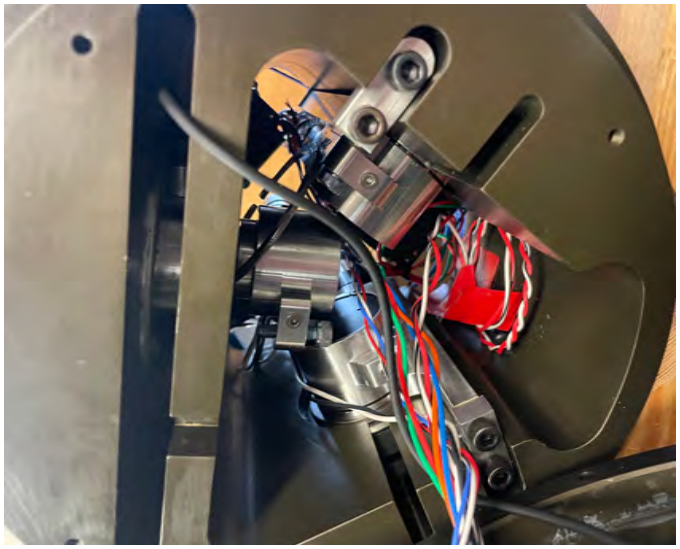

Figure 10: A view inside the rotor hub showing installed shaft seals, load cell, and gear boxes. The challenges with designing and installing these components ultimately determined the required diameter of the AFT.

set screw. One of the three blades is equipped with an ATI Mini58 six-axis load cell. The back end of the hub is sealed by a mounting plate with an ATI Mini58 load cell coupled to a fixed shaft that translates the rotary motion to the nacelle shaft. Bulkhead connectors (SubConn BH and MCBH) are installed at the base of the hub into the nacelle.

2.4 Controls

The Axial Flow Turbine control software is written in C++ utilizing the Qt application framework for the main control system and graphical user interface (GUI). The control system runs on a real-time Linux kernel, with a 1 kHz real-time control and data logging cycle. The system communicates with three Maxon motor controllers over a CAN bus to provide blade pitch control, and two ATI 6-axis load cells to capture blade and rotor forces and torques during operation. The main rotor is driven by the VFD, which is controlled through MODBUS RTU. Rotor position and speed are recorded using a RLS quadrature encoder. The control software records blade pitch position and VFD commands (set points), encoder position, and load cell data at 1 kHz to binary log files. System setpoints can be controlled manually, or a range of setpoints, step sizes, and dwell times can be entered into the GUI (Fig. 11) for automated test runs, with automatic log file rotation corresponding to each system setpoint for ease of data analysis.

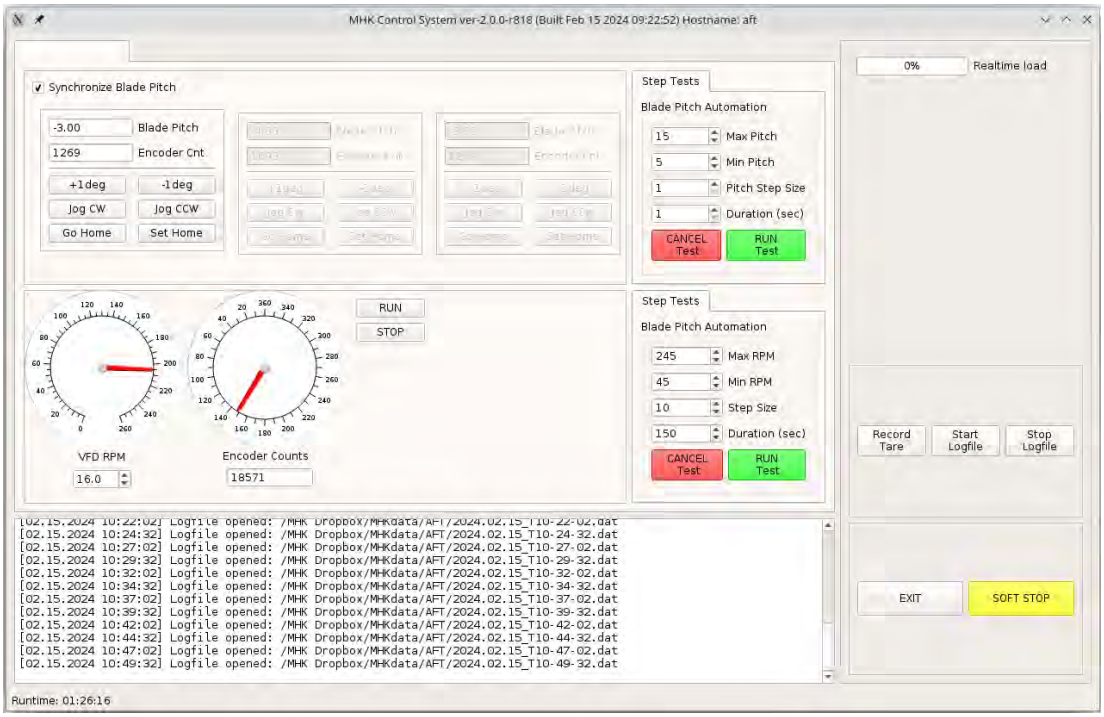

Figure 11: The graphical user interface for the AFT system.

Each log file (binary, .dat) contains all of the data recorded by the control software. Thus, each line in the .dat file contains six torques and six forces from the load cells, the VFD speed command, shaft encoder position, and blade pitch position. A custom MATLAB script is used to unpack the binary files for further processing.

2.5 System Mounting

The aft sections of the AFT were fabricated with a series of holes spaced along horizontal members welded to the exterior of the housing (Fig. 6). To mount the system on the RDL gantry, a shaft with a pivot joint and coupling with two holes is aligned with each of the two hub sections on the AFT. These aluminum pipes run to a series of clamps that can be used to secure the unit to cross members of the RDL gantry. The different holes, pivot joints, and sliding clamps allow the unit's position and attitude to be modified during installation. The AFT standard configuration is horizontal installation (Fig. 12). By modifying the clamp locations and mounting positions on the AFT, the unit can be pitched. The purpose of this flexible-pitch mounting is to replicate conditions for off-axis flow in a yaw-controlled system while allowing for relatively easy installation on RDL.

Figure 12: Photo of the field-scale AFT installed on RDL in preparation for system commissioning.

3 TESTING AND RESULTS

Field testing with the AFT typically involves 4–8 hr of vessel time per day, with an expected 60–80 min round-trip for transportation between the dock and Lake Washington. Once on the lake, the turbine is lowered into the water, tare measurements are recorded with the vessel out of gear to bias the load cell measurements, and the vessel is driven at speeds of 2–5 knots (1–2.5 m/s) over ground while acquiring data over a range of rotation rates, preset pitch angles, or turbine incline angles. Vessel speeds less than 2 knots (≈1 m/s) are not recommended at the present time due to lower signal to noise ratios on the load cell measurements and the difficulty in maintaining low vessel speeds, particularly in stronger winds.

For freestream velocity measurements, a Nortek acoustic Doppler velocimeter (ADV) is installed 1.4 m in front of the rotor plane. Other sampling parameters including the sampling rate, nominal velocity range, and sampling volume can be configured within the bounds of the software. The ADV is set to record continuously for the duration of testing. Because the ADV data are collected external to the rest of the data acquisition software, the timestamps on the ADV data files are used in post-processing to match the appropriate time series of inflow and load cell measurements. A 150 s sample of the horizontal inflow speed measured from the ADV is shown in Fig. 13.

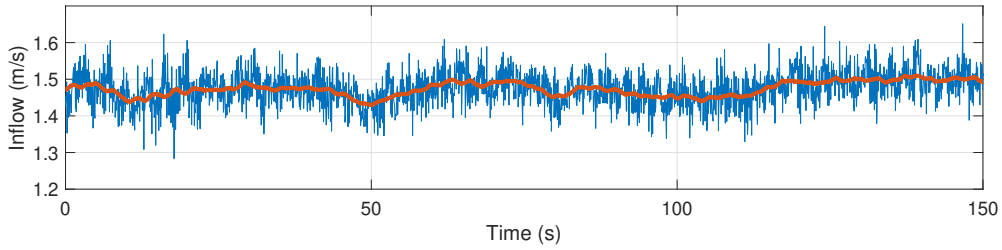

Figure 13: Representative time series of the horizontal flow speed calculated from the X and Y measurements from the ADV, sampled at 16 Hz. Orange line shows the 5-s moving average.

Non-dimensional metrics of turbine performance and dynamic loading are typically characterized over a range of tip-speed ratios, λ, defined as $\lambda = \omega r/U$, where ω is the rotation rate, r is the turbine radius, and U is the freestream velocity. For this characterization, we hold the vessel speed (and, therefore, U) approximately constant and vary the rotation rate over a range of set points expected to produce positive mechanical power. For a single sweep through multiple rotation rates, the minimum, maximum, step size, and duration at each set point is specified in the data acquisition software. Prior to the sweep, a tare measurement is recorded in still water to bias

the load cell measurements. This involves rotating the turbine rotor at 12–16 RPM (the lowest possible set point to overcome friction in the system) for 2 min to capture the tare measurements at different blade positions. Drift on the load cell measurements is normal and expected, so tares are recorded regularly throughout the day. Typically, this is done once before each sweep through multiple rotation rates, but the recommended frequency of the tare measurement depends on the expected loads and operating conditions and the acceptable experimental uncertainty.

Sample time series of the rotor thrust, rotor torque, and blade thrust for $U = 1.7\,\mathrm{m/s}$ and $\omega = 2.6$ revolutions per second (RPS) are shown in Fig. 14. The frequency spectrum of the blade thrust in Fig. 15 demonstrates that the only dominant frequencies present are the blade passing frequency and associated harmonics. The frequency spectra of the blade or rotor loads can also be used as a reliable method of determining rotation rate if encoder data are not available.

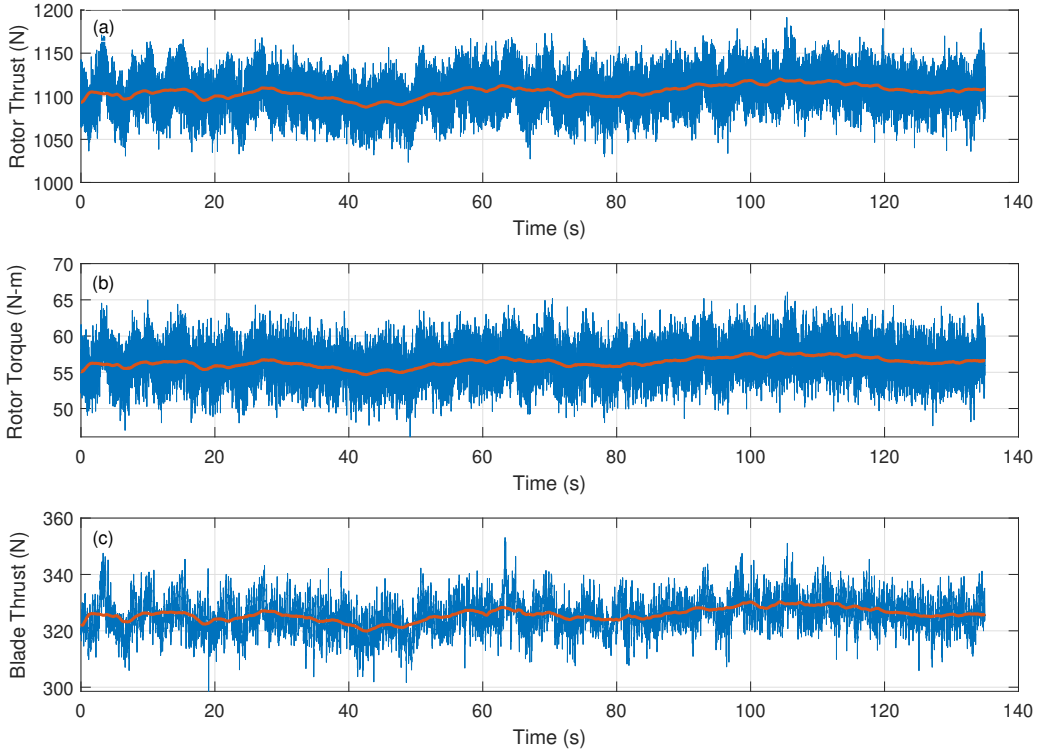

Figure 14: Representative time series of the (a) rotor thrust and (b) rotor torque measured from the six-axis load cell on the drive shaft, as well as (c) the streamwise force on a single blade measured from the six-axis load cell at the root of a blade. Orange lines show the 5-s moving averages. Sample data were taken in $U = 1.7\,\mathrm{m/s}$ for $\omega = 2.6$ RPS.

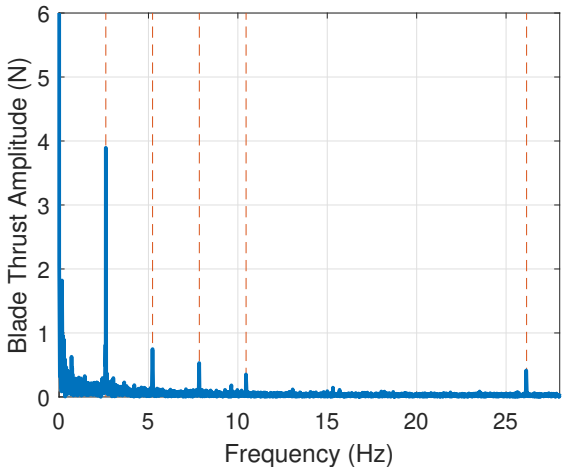

Figure 15: Frequency spectrum of the blade thrust measured from the six-axis load cell at the root of the key blade. The axes limits are set to emphasize the blade passing frequency and associated harmonics, which are indicated by the dotted lines.

Sample turbine performance curves achieved through field testing are shown in Fig. 16, including normalized power and thrust as a function of tip-speed ratio. Mechanical power, calculated from the rotation rate and measured torque, is normalized by the kinetic power available in the inflow to produce the power coefficient, C_P:

$$C_P = \left\langle \frac{\tau\omega}{0.5\rho A U_m^3} \right\rangle, \tag{1}$$

where τ is the torque measured by the load cell on the drive shaft, A is the rotor swept area, ρ is water density, and U_m is the 5-s moving average of the horizontal ADV measurement. Thrust, T, is normalized by the dynamic pressure force across the rotor swept area to produce the thrust coefficient, C_T:

$$C_T = \left\langle \frac{T}{0.5\rho A U_m^2} \right\rangle. \tag{2}$$

The spanwise and chordwise centers of pressure on the blade may also be of interest because of their effect on hydrodynamic performance, structural integrity, and blade deformation. Shown in Fig. 17, these can be calculated using the measurements from the six-axis load cell at the root of the key blade from the following equations:

$$M_{pitch} = F \cdot R_{chord}, \text{ and} \tag{3}$$

$$M_{bend} = F \cdot R_{span}, \tag{4}$$

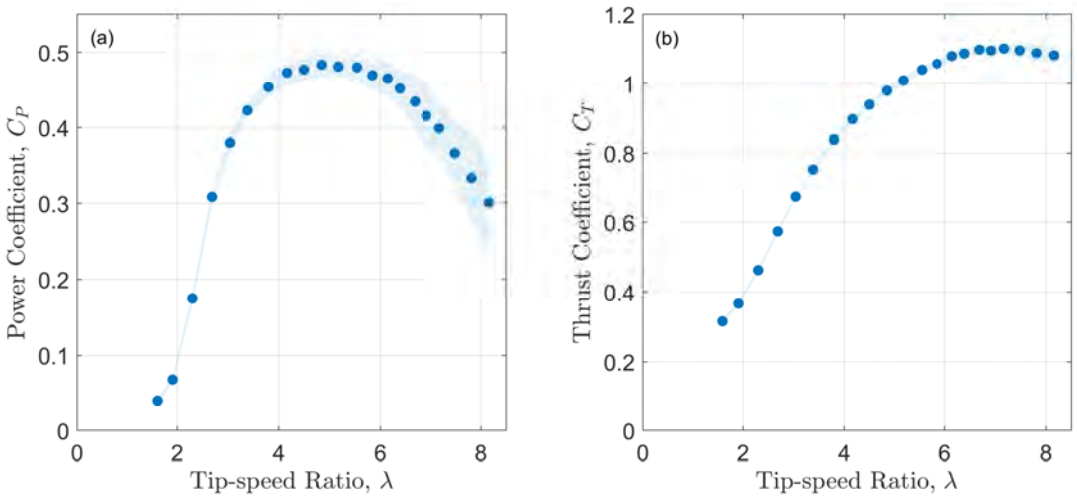

Figure 16: Power and thrust coefficients as a function of tip-speed ratio, tested in 1.7 m/s flow. The shaded regions represent the interquartile range of measurements.

where M_{pitch} and M_{bend} are the pitching and flapwise bending moments, F is the flapwise force on the blade, and R_{chord} and R_{span} are the pitching and flapwise bending moment arms. M_{pitch}, M_{bend}, and F are all measured directly from the blade load cell. R_{chord} is equivalent to the chordwise center of pressure relative to the pitching axis (Fig. 17a), and R_{span} when summed with the distance between the sensor head and the drive shaft is equivalent to the spanwise center of pressure relative to the rotor axis (Fig. 17b).

Phase-averaged loads are also available using the encoder data. An example is shown in Fig. 18 for blade thrust, where each load measurement is binned according to the corresponding azimuthal position of the rotor and averages for each 10°-wide bin are reported. This is particularly useful in cases where the inflow is yawed or non-uniform to understand individual blade load fluctuations. In this case, intra-cycle fluctuations are small (3 %) because the flow is largely uniform across the rotor plane and with no yaw.

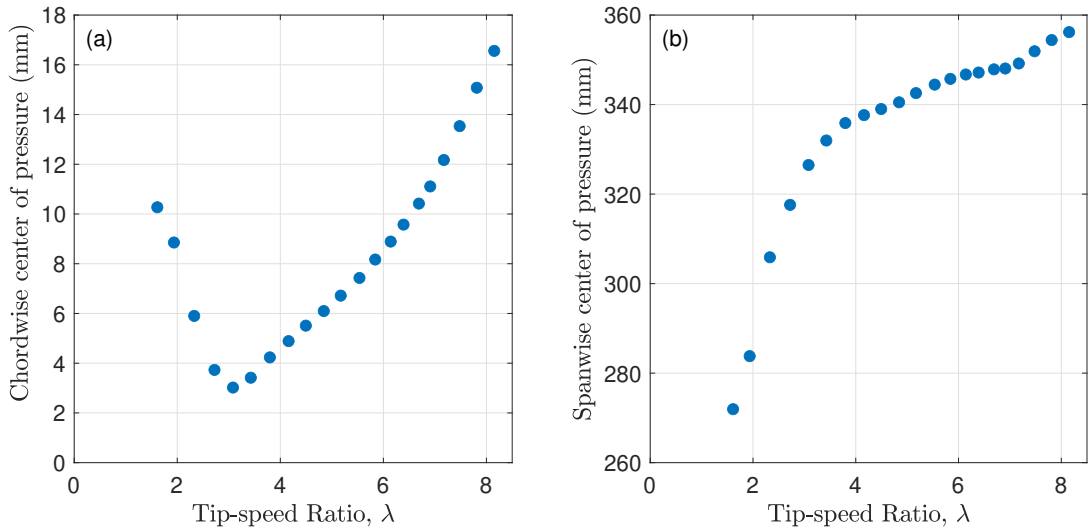

Figure 17: Calculations of the (a) chordwise and (b) spanwise centers of pressure on the blade as a function of tip-speed ratio. The chordwise location is relative to the pitching axis (also the quarter-chord), where positive values are closer to the trailing edge. The spanwise location is relative to the rotor's axis, where 80 mm is the location of the blade root and 500 mm is the location of the blade tip.

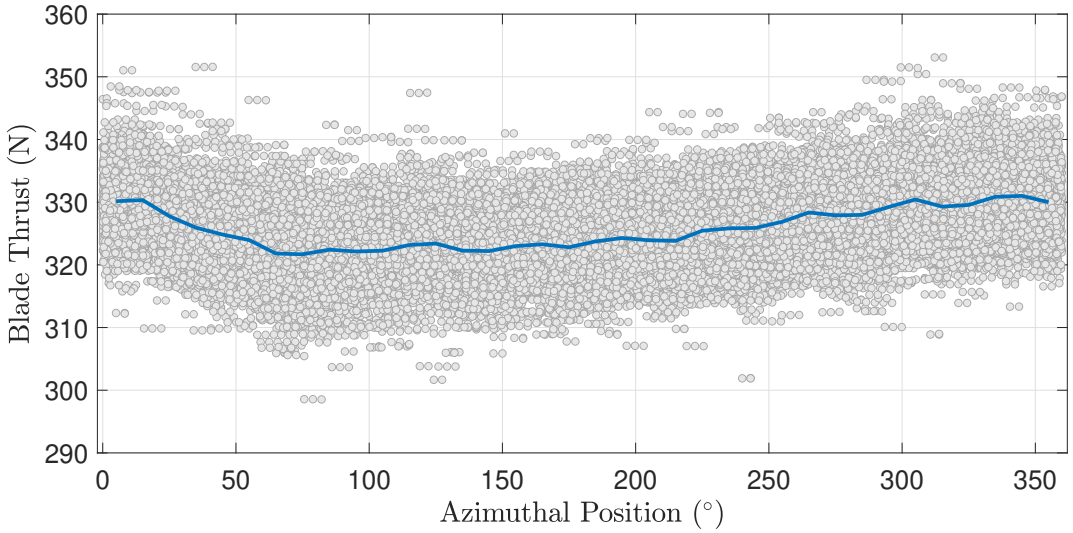

Figure 18: Sample measurements of blade thrust phase-averaged into 10°-wide bins. Individual measurements are shown in grey. The 0° position corresponds to when the blade is oriented vertically, at the top of the rotation.

4 SUMMARY

The APL-UW axial flow turbine was designed and fabricated to extend the University of Washington's capabilities for testing and characterization of axial flow turbines from the laboratory to field-scale. It has been used to measure the performance and loads generated by "rigid" and passive adaptive blades operated across a range of inflow conditions, tip-speed ratios, and blade pitches. In addition, similar measurements under fixed non-normal inflow conditions representing a yawed turbine have been performed.

A summary of key specifications is provided in Table 1. Ongoing research activities include the design, fabrication, and testing of additional passive adaptive blade designs. In addition, APL-UW continues to develop AFT capabilities and is actively pursuing the development of a swappable, fixed-pitch hub equipped with a fiberoptic interrogator for strain sensing of specially developed blades. These capabilities will further extend our ability to perform research related to small, field-scale axial flow turbines.

Table 1: Turbine specifications: rotor thrust and torque limitations are associated with the six-axis load cells. The 260 RPM limit on rotation rate will extend to higher rotation rates with the fixed-pitch hub now in development.

Parameter	Value
Rotor diameter	$\leq$1.6 m
Rotor rotation rate	14–260 RPM
Rotor thrust	$\leq$6800 N
Rotor torque	$\leq$120 N m
Yaw angle	$\leq$25°
Blade pitch	$\pm$90°
Inflow	$\leq$2.5 m/s

REFERENCES

[1] K. Van Ness, C. Hill, A. Aliseda, and B. Polagye. Demonstration of blade pitch control for horizontal-axis tidal turbines. In *Proc. 13th European Wave and Tidal Energy Conference, Napoli, Italy, 1–6 September*, 2019. doi: 10.1109/AUV.1994.518601.

[2] K. Van Ness, C. Hill, J. Burnett, A. Aliseda, and B. Polagye. Experimental comparison of blade pitch and speed control strategies for horizontal-axis current turbines. *J. Ocean. Eng. Mar. Energy*, 7:83–96, 2021. doi: 10.1007/s40722-021-00188-w.

[3] K. Van Ness, A. Aliseda, and B. Polagye. Experimental comparison of passive adaptive blade pitch control strategies for an axial-flow current turbine. *J. Ocean. Eng. Mar. Energy*, 10: 105–123, 2023. doi: 10.1007/s40722-023-00302-0.